

SEMI-SUPERVISED DOMAIN ADAPTATION FOR WILDFIRE DETECTION

JooYoung Jang^{1,2} Youngseo Cha¹ Jisu Kim¹ SooHyung Lee¹ Geonu Lee¹
Minkook Cho¹ Young Hwang¹ Nojun Kwak^{2*}

¹Alchera, South Korea ²Seoul National University, South Korea

jyjang1090@snu.ac.kr, {ys.cha, js.kim, _shlee, gu.lee}@alcherainc.com, nojunk@snu.ac.kr

ABSTRACT

Recently, both the frequency and intensity of wildfires have increased worldwide, primarily due to climate change (Sathishkumar et al., 2023). In this paper, we propose a novel protocol for wildfire detection, leveraging semi-supervised Domain Adaptation for object detection, accompanied by a corresponding dataset designed for use by both academics and industries. Our dataset encompasses 30 times more diverse labeled scenes for the current largest benchmark wildfire dataset, HPWREN (2000), and introduces a new labeling policy for wildfire detection. Inspired by Liu et al. (2018), we propose a robust baseline, Location-Aware Object Detection for Semi-Supervised Domain Adaptation (LADA), utilizing a teacher-student (Liu et al., 2021) based framework capable of extracting translational variance features characteristic of wildfires. With only using 1% target domain labeled data, our framework significantly outperforms our source-only baseline by a notable margin of 3.8% in mean Average Precision on the HPWREN wildfire dataset. Our dataset is available at <https://github.com/BloomBerry/LADA>.

1 INTRODUCTION

Wildfires contribute to and are exacerbated by global warming, leading to significant economic losses and ecological damage (Sathishkumar et al., 2023; Lindsey & Dahlman, 2020). Such impacts can be mitigated through the early detection of wildfires, enabling firefighters to intervene promptly. For effective mitigation, wildfire detection systems must achieve high accuracy and maintain low false positive rates (Ranadive et al., 2022).

However, applying fire detection in real-world scenarios present challenges, including a domain shift between the training and testing environments that can degrade detection performance (Yoo et al., 2022). Even worse, acquiring a large volume of labeled data for the target domain is particularly challenging for infrequent events like wildfires (Kim et al., 2022). To address these challenges, this paper introduces a new protocol, semi-supervised domain adaptation(SSDA) for wildfire detection. To the best of our knowledge, this is the first paper to apply SSDA for object detection task. As depicted in Fig.1, SSDA is a combination of semi-supervised learning (SSL) and unsupervised domain adaptation (UDA) task. It uses large amount of source domain images, while uses minimal set of target labeled images alongside a substantial corpus of target unlabeled images. SSDA setting is practical for real-world application considering labeling cost and performance. (Yu & Lin, 2023)

*corresponding author: Nojun Kwak (nojunk@snu.ac.kr)

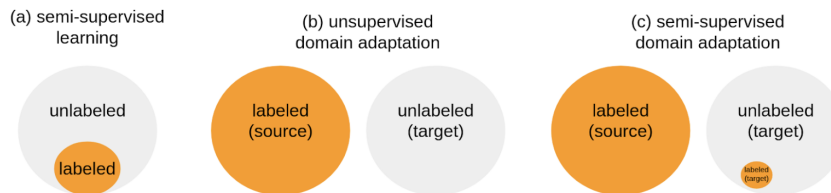


Figure 1: semi-supervised Domain Adaptation

This work makes two primary contributions. First, we introduce new labels for wildfire detection tasks, increasing label diversity by thirtyfold compared to existing labels within the HPWren dataset, as in Table 3. We classified source domain as previous publicly available labels and target domain as new labeled set we suggested in this paper. Second, we present a novel approach to learn translational variance characteristics of wildfires called Location-Aware Semi-Supervised Domain Adaptation (LADA) framework, which integrates Coordinate Convolution (Liu et al., 2018) with a scale-aware Faster R-CNN (Chen et al., 2021b). Our result demonstrate enhanced performance across various SSDA protocols from current state-of-the-art UDA framework (Hoyer et al., 2023).

Related work. SSDA approach seeks to reduce the domain-gap between source and target using consistency regularization loss (Yu & Lin, 2023), or use cutmix augmentation for domain-mixing loss (Chen et al., 2021a). However, those methods neither applied for object detection task. Our method uses consistency regularization loss using masked augmentation similar to (Hoyer et al., 2023).

2 METHODS

2.1 PROPOSED DATASET

In this paper, we propose a refined set of labels for the HPWREN (2000) dataset. This dataset serves as a benchmark for wildfire detection tailored to individual researchers. However, direct application of this benchmark for research encounters two primary obstacles. First, the diversity and quality of the labels are limited, leading to potential overfitting issues. Specifically, the dataset comprises only 609 labeled images across 9 scenes. Second, the practice of labeling smoke with separated bounding boxes demands considerable time and efforts for annotation. We have discovered that merging these bounding boxes not only simplifies the labeling process but also improves detection performance, as illustrated in Fig. 2. Detailed results are presented in Section 3.

To address these challenges, we introduce a new benchmark for semi-supervised domain adaptation in object detection, detailed in Table 1. Inspired by Li et al. (2023), we propose three protocols, 0.5%, 1.0%, and 3.0%, representing the ratio of labeled data in the target domain relative to the total dataset. In this benchmark, the source domain comprises 9 sub-directories with labels available on the HPWREN (2000) homepage, while 274 sub-directories are designated as the target domain. This configuration results in a domain shift, as the source and target domains do not share a common environment.

2.2 LOCATION-AWARE SEMI-SUPERVISED DOMAIN ADAPTATION

Preliminary. In this study, we tackle the challenge of early wildfire detection by leveraging object detection frameworks (Chen et al., 2021b). Image samples are denoted by $\mathbf{x}_s = (x_i)_{i=1}^{N_s}$, $\mathbf{x}_{tl} = (x_i)_{i=1}^{N_{tl}}$

Table 1: Number of sub-directories, and labels for HPWREN dataset

	Previous labels	Proposed labels	Total HPWREN
Number of sub-directories	9	283	342
Number of images	609	2,575	27,174

Table 2: semi supervised domain adaptation for wildfire detection protocol

	source	target 0.5%	target 1.0%	target 3.0%	target val
foreground images	309	44	94	257	451
background images	300	58	111	359	630
total images	609	102	205	616	1,081

and corresponding bounding-box labels $\mathbf{y}_s = (y_i)_{i=1}^{N_s}$, $\mathbf{y}_{tl} = (y_i)_{i=1}^{N_{tl}}$ are utilized as input to the model, where N_s, N_{tl} is the number of labeled samples for source and target domain each. The label consists of class and bounding boxes $y_i = (c, x, y, w, h)$ where c, x, y, w represents class index, center points, width and height of the box. In addition, the pseudo bounding-box labels $\mathbf{u} = (u_i)_{i=1}^{N_{tu}}$ are constructed when the confidence score is bigger than the upper threshold $p_u > \tau_u$, or smaller than the lower threshold $p_u < \tau_l$ where τ_u, τ_l , and N_{tu} represents upper, lower confidence threshold, and number of unlabeled target samples, each.

Pseudo Labeling. We utilize large amount of unlabeled target data with a teacher-student paradigm (Liu et al., 2021) augmented with Masked Image Consistency (MIC) Loss (Hoyer et al., 2023). Built upon that, we changed pseudo label filter to use reliable background images implemented by very low probability score in order to train background images, as shown in equation 1. \hat{y}_i represents i_{th} unlabeled target sample index. We used $\tau_u = 0.8, \tau_l = 0.05$ for all of our experiments. We find that it is helpful especially for 0.5%, 1.0% SSDA protocols which lacks of highly reliable positive images. Further information is in Appendix C.

Translation Variance Features. Wildfires typically don't occur in specific area, such as skies or lakes, or it shows a location-dependent shapes. For instance, they seldom occur in the upper portion of the images, which are predominantly occupied by the sky, while many of them has conical shape, expanding vertically. In order to utilize such characteristics, the Coordinate Convolution layer (Liu et al., 2018) was incorporated into both the Feature Pyramid Network (FPN) (Lin et al., 2017) and the Region Proposal Network (RPN) (Ren et al., 2015), as illustrated in Fig. 3. Coordinate convolution layer embed coordinate information through two channels, x and y to the original convolution layers, and the new added channels enable the model to capture such translational variance features at a minimal computational cost. We didn't add Coordinate convolution layer into the backbone as suggested in the (Liu et al., 2018), since it did not show good performance.

Location Aware Domain Adaptation. The comprehensive diagram of our training process is depicted in Fig. 4. The student model is trained using both supervised and unsupervised losses, whereas the teacher model is periodically updated through an Exponential Moving Average. Unsupervised losses consist of masked image consistency loss, pseudo label based Cross entropy loss, and adversarial loss. The former allows the model to learn consistent output from masked image to original image, which allows the model to learn robust predictions even in such randomly masked images. Pseudo labeling loss, on the other hand, make use of a large amount of unlabeled target images to train as supervised learning. Finally, adversarial loss aligns the source and target domain features in the backbone in order to reduce domain gap in three levels. More training detail information is available in Appendix B.

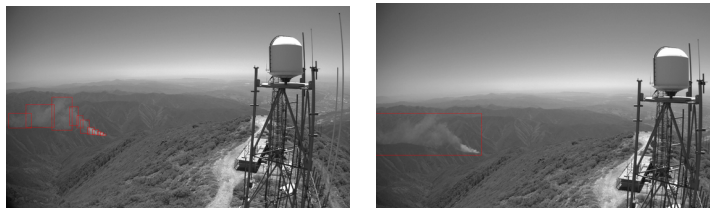


Figure 2: Original HPWREN labeled image (Left) vs. Proposed labeled image (Right)

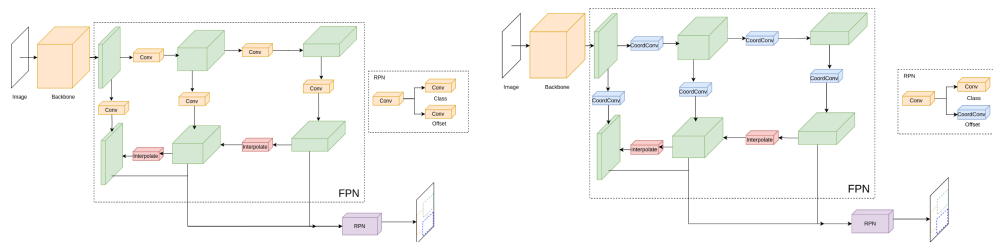


Figure 3: Location Aware semi-supervised Domain Adaptation Network. We omitted the second stage regression and classification heads for simplicity.

$$\begin{cases} \hat{p}_i > \tau_u \\ \hat{p}_i < \tau_l \end{cases} \quad (1)$$

3 RESULTS

Our model is trained in two stages. In the first stage, the training exclusively utilized source data. In the subsequent stage, a combination of labeled source data, labeled target data, and unlabeled data was employed. We conducted an initial comparison between the original HPWREN labels and our proposed labeling approach. As detailed in Table 3, our approach, which utilizes merged bounding boxes, improves up to 10.9 mean Average Precision@0.5:0.95 (mAP) over the original labels. Based on these results, we advocate for the adoption of our merged bounding box labeling strategy in wildfire detection.

Table 3: Comparison between original & proposed labeling policy at mAP/mAP@0.5

	0.5%	1.0%	3.0%
original label	1.5/7.0	2.8/12.9	7.9/29.6
merged label	7.9/24.0	10.2/31.5	18.8/48.4

As presented in Table 4, our model surpasses the performance of the model proposed by Chen et al. (2021b) in the source-only protocol. This protocol exclusively utilizes the source dataset for training and subsequently validates the model on the target validation dataset. Our model also outperforms Hoyer et al. (2023) in semi-supervised Domain Adaptation protocols. The results indicate that our proposed method catches the translational variance features of wildfire well, leading to better generalization performance.

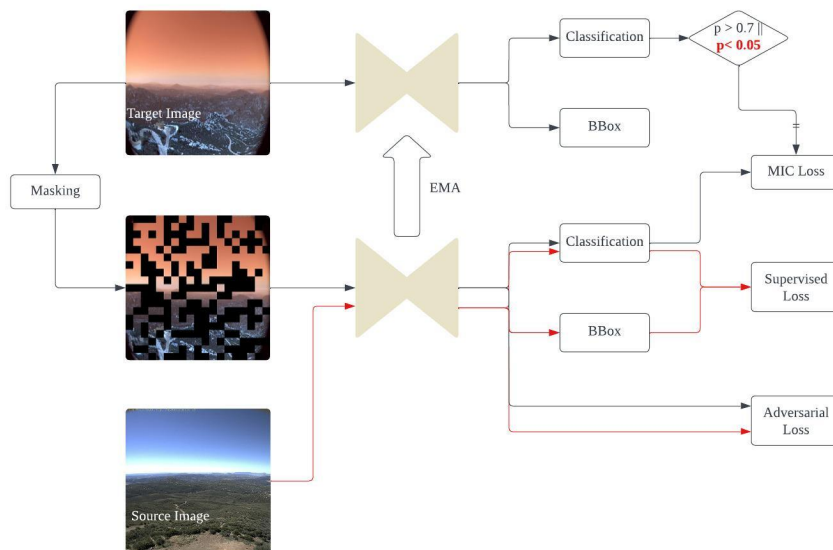


Figure 4: Overall Diagram of our training process. We also use background images for training.

Type	Methods	Labeled target images		
		0.5%	1.0%	3.0%
Source-only	SADA (Chen et al., 2021b)	6.9/21.9	9.7/28.7	17.8/48.0
	LADA(ours)	7.9/24.0	10.2/31.5	18.8/48.4
SSDA	SADA (Hoyer et al., 2023)	9.7/27.3	12.3/34.9	20.4/53.0
	LADA(ours)	10.0/29.1	14.0/38.0	20.9/52.3

Table 4: Comparison of source-only and SSDA results. (mAP/mAP@0.5)

4 CONCLUSION

In this paper, we propose a novel benchmark utilizing semi-supervised domain adaptation for object detection, designed to benefit both academia and industry. Our labeling approach introduces a diversity that is thirtyfold greater than that of existing wildfire benchmarks and presents a new labeling policy tailored for wildfire detection. Furthermore, we establish a robust baseline for this benchmark, named LADA (Location-Aware Semi-Supervised Domain Adaptation), distinguished by its capability to capture translational variance features pertinent to wildfire detection.

5 ACKNOWLEDGEMENTS

This work was supported by NRF grant (2022R1A5A7026673) funded by MSIT, Korean Government.

REFERENCES

- Shuaijun Chen, Xu Jia, Jianzhong He, Yongjie Shi, and Jianzhuang Liu. Semi-supervised domain adaptation based on dual-level domain mixing for semantic segmentation. *CVPR*, 2021a.
- Yuhua Chen, Haoran Wang, Wen Li, Christos Sakaridis, Dengxin Dai, and Luc Van Gool. Scale-aware domain adaptive faster r-cnn. *IJCV*, 2021b.
- Lukas Hoyer, Dengxin Dai, Haoran Wang, and Luc Van Gool. Masked image consistency for context-enhanced domain adaptation. *CVPR*, 2023.
- HPWREN. The high performance wireless research and education network. <http://hpwren.ucsd.edu/>, 2000.
- JongMok Kim, JooYoung Jang, Seunghyeon Seo, Jisoo Jeong, Jongkeun Na, and Nojun Kwak. Mum : Mix image tiles and unmix feature tiles for semi-supervised object detection. *CVPR*, 2022.
- Jichang Li, Guanbin Li, and Yizhou Yu. Adaptive betweenness clustering for semi-supervised domain adaptation. *TIP*, 2023.
- Tsung-Yi Lin, Piotr Dollár, Ross Girshick, Kaiming He, Bharath Hariharan, and Serge Belongie. Feature pyramid networks for object detection. *Institute of Electrical and Electronics Engineers*, 2017.
- Rebecca Lindsey and LuAnn Dahlman. Climate change: Global temperature. *Available online: climate.gov*, 2020.
- Rosanne Liu, Joel Lehman, Piero Molino, Felipe Petroski Such, Eric Frank, Alex Sergeev, and Jason Yosinski. An intriguing failing of convolutional neural networks and the coordconv solution. *NIPS*, 2018.
- Yen-Cheng Liu, Chih-Yao Ma, Zijian He, Chia-Wen Kuo, Kan Chen, Peizhao Zhang, Bichen Wu, Zsolt Kira, and Peter Vajda. Unbiased teacher for semi-supervised object detection. *arXiv preprint arXiv:2102.09480*, 2021.
- Omkar Ranadive, Jisu Kim, Serin Lee, Youngseo Cha, Heechan Park, Minkook Cho, and Young Hwang. Image-based early detection system for wildfires. *NIPS*, 2022.
- Shaoqing Ren, Kaiming He, Ross Girshick, and Jian Sun. Faster r-cnn: Towards real-time object detection with region proposal networks. *NIPS*, 2015.
- Veerappampalayam Easwaramoorthy Sathishkumar, Jaehyuk Cho, Malliga Subramanian, and Obuli Sai Naren. Forest fire and smoke detection using deep learning-based learning without forgetting. *Fire Ecology*, 2023.
- Jayeon Yoo, Inseop Chung, and Nojun Kwak. Unsupervised domain adaptation for one-stage object detector using offsets to bounding box. *ECCV*, 2022.
- Yu-Chu Yu and Hsuan-Tien Lin. Semi-supervised domain adaptation with source label adaptation. *CVPR*, 2023.

A DATASET

This section will give more information of HPWREN dataset, and how source and target domain has been composed. Each image files are named as equation 2.

$$YYYYMMDD_fireName_cameraName \quad (2)$$

We defined domain shift based on equation 2, and simply splitted train and validation set. We splitted target validation set and target train set with 5%, 95% by random sampling. We also random sampled 0.5%, 1.0%, 3.0% target labeled dataset among 95% of target train dataset for each semi-supervised domain adaptaion protocols. Sub-directories for source domain and target domain are summarized in Table 5 to 16. However, we noticed that users could also split based on customized domain shift scenario. For example, we illustrate defining domains with **cameraName** in Equation 2. It is summarized in Table 17 to 19.

Scene Description	# of Imgs	Scene Description	# of Imgs
20160604_FIRE_rm-n-mobo-c	81	20160604_FIRE_smer-tcs3-mobo-c	81
20160619_FIRE_lp-e-iqeye	41	20160619_FIRE_om-e-mobo-c	81
20160619_FIRE_pi-s-mobo-c	81	20160711_FIRE_ml-n-mobo-c	81
20160718_FIRE_lp-n-iqeye	41	20160718_FIRE_mg-s-iqeye	41
20160718_FIRE_mw-e-mobo-c	81		

Table 5: Scenes composed for source domain dataset by equation 2

Scene Description	# of Imgs	Scene Description	# of Imgs
20160722_FIRE_mg-s-iqeye	41	20170708_Whittier_syp-n-mobo-c	81
20160722_FIRE_mw-e-mobo-c	81	20170708_Whittier_syp-n-mobo-m	80
20161113_FIRE_bl-n-mobo-c	81	20170711_FIRE_bl-e-mobo-c	81
20161113_FIRE_bm-n-mobo-c	81	20170711_FIRE_bl-s-mobo-c	81
20161113_FIRE_bm-w-mobo-c	81	20170711_FIRE_bm-s-mobo-c	64
20170519_FIRE_rm-w-mobo-c	81	20170711_FIRE_sdsc-e-mobo-c	81
20170520_FIRE_lp-s-iqeye	81	20170711_FIRE_sm-n-mobo-c	81
20170520_FIRE_om-s-mobo-c	55	20170713_FIRE_smer-tcs8-mobo-c	77
20170520_FIRE_pi-s-mobo-c	81	20170722_FIRE_bm-n-mobo-c	81
20170520_FIRE_pi-w-mobo-c	81	20170722_FIRE_hp-e-mobo-c	81
20170609_FIRE_sm-n-mobo-c	81	20170722_FIRE_mg-n-iqeye	81
20170613_FIRE_bh-w-mobo-c	81	20170722_FIRE_so-s-mobo-c	81
20170613_FIRE_hp-n-mobo-c	81	20170807_FIRE_bh-n-mobo-c	78
20170625_BBM_bm-n-mobo	81	20170821_FIRE_lo-s-mobo-c	81
20170625_FIRE_mg-s-iqeye	81	20170826_FIRE_tp-s-mobo-c	81

Table 6: Scenes composed for target domain dataset by equation 2 (Part. 1)

An example of our proposed labels are show in Fig. 5.

Scene Description	# of Imgs	Scene Description	# of Imgs
20170901_FIRE_om-s-mobo-c	81	20171017_FIRE_smer-tcs3-mobo-c	78
20170927_FIRE_smer-tcs9-mobo-c	81	20171021_FIRE_pi-e-mobo-c	81
20171010_FIRE_hp-n-mobo-c	81	20171026_FIRE_rm-n-mobo-c	81
20171010_FIRE_hp-w-mobo-c	81	20171026_FIRE_smer-tcs8-mobo-c	81
20171010_FIRE_rm-e-mobo-c	81	20171207_FIRE_bh-n-mobo-c	81
20171016_FIRE_sdsc-e-mobo-c	81	20171207_FIRE_bh-w-mobo-c	77
20171017_FIRE_smer-tcs3-mobo-c	78	20171207_FIRE_smer-tcs8-mobo-c	81
20171021_FIRE_pi-e-mobo-c	81	20171207_Lilac_rm-s-mobo	81
20171026_FIRE_rm-n-mobo-c	81	20180504_FIRE_bh-n-mobo-c	81
20171026_FIRE_smer-tcs8-mobo-c	81	20180504_FIRE_rm-n-mobo-c	81
20171207_FIRE_bh-n-mobo-c	81	20180504_FIRE_smer-tcs10-mobo-c	81
20171207_FIRE_bh-w-mobo-c	77	20180504_FIRE_smer-tcs8-mobo-c	81
20171207_FIRE_smer-tcs8-mobo-c	81	20180517_FIRE_rm-n-mobo-c	81
20171207_Lilac_rm-s-mobo	81	20180517_FIRE_smer-tcs10-mobo-c	81
20180504_FIRE_bh-n-mobo-c	81	20180522_FIRE_rm-e-mobo-c	81
20180504_FIRE_rm-n-mobo-c	81	20180602_Alison_sp-s-mobo-c	81
20180504_FIRE_smer-tcs10-mobo-c	81	20180602_Alison_sp-w-mobo-c	81
20180504_FIRE_smer-tcs8-mobo-c	81	20180602_FIRE_rm-n-mobo-c	81
20180517_FIRE_rm-n-mobo-c	81	20180602_FIRE_smer-tcs8-mobo-c	81
20180602_FIRE_smer-tcs9-mobo-c	81	20180603_FIRE_bl-s-mobo-c	81

Table 7: Scenes composed for target domain dataset by equation 2 (Part. 2)

Scene Description	# of Imgs	Scene Description	# of Imgs
20180603_FIRE_rm-w-mobo-c	81	20180606_FIRE_lo-s-mobo-c	81
20180603_FIRE_smer-tcs8-mobo-c	81	20180606_FIRE_ml-s-mobo-c	81
20180603_FIRE_smer-tcs9-mobo-c	81	20180606_FIRE_pi-e-mobo-c	81
20180603_FIRE_sm-n-mobo-c	81	20180611_fallbrook_rm-w-mobo-c	81
20180603_FIRE_sm-w-mobo-c	81	20180612_FIRE_rm-w-mobo-c	81
20180605_FIRE_rm-w-mobo-c	81	20180612_FIRE_smer-tcs9-mobo-c	81
20180605_FIRE_smer-tcs9-mobo-c	81	20180614_Bridle_hp-n-mobo-c	81
20180614_FIRE_hp-s-mobo-c	68	20180704_Benton_hp-n-mobo-c	81
20180614_Hope_wc-e-mobo-c	81	20180706_FIRE_sm-e-mobo-c	81
20180706_FIRE_sm-n-mobo-c	70	20180706_FIRE_wc-e-mobo-c	69
20180706_West_lp-n-mobo-c	81	20180717_otay_om-s-mobo-c	81
20180718_FIRE_syp-w-mobo-c	81	20180719_Skyline_sp-n-mobo-c	81
20180720_Cinnamon_wc-e-mobo-c	81	20180720_FIRE_syp-w-mobo-c	81
20180723_FIRE_tp-e-mobo-c	81	20180725_Cranston_hp-n-mobo-c	81

Table 8: Scenes composed for target domain dataset by equation 2 (Part. 3)

Scene Description	# of Imgs	Scene Description	# of Imgs
20180725_Cranston_sp-e-mobo-c	81	20180806_FIRE_mg-s-mobo-c	78
20180725_FIRE_smer-tcs10-mobo-c	81	20180806_FIRE_vo-w-mobo-c	81
20180726_FIRE_so-n-mobo-c	81	20180806_Holy_sp-s-mobo-c	72
20180726_FIRE_so-w-mobo-c	81	20180806_Holy_sp-s-mobo-m	73
20180727_FIRE_bh-n-mobo-c	81	20180809_FIRE_bh-s-mobo-c	80
20180727_FIRE_bh-s-mobo-c	81	20180809_FIRE_bl-e-mobo-c	81
20180727_FIRE_bl-e-mobo-c	81	20180809_FIRE_mg-w-mobo-c	81
20180727_FIRE_mg-w-mobo-c	81	20180813_FIRE_bh-s-mobo-c	81
20180727_FIRE_wc-n-mobo-c	81	20180813_FIRE_bl-n-mobo-c	81
20180728_FIRE_rm-w-mobo-c	81	20180813_FIRE_mg-w-mobo-c	81
20180728_FIRE_smer-tcs9-mobo-c	81	20180827_Holyflareup_sp-e-mobo-c	81
20180910_FIRE_smer-tcs8-mobo-c	81	20180919_FIRE_rm-e-mobo-c	81
20181112_house_wc-n-mobo-c	71	20190529_94Fire_lp-s-mobo-c	81
20190529_94Fire_om-n-mobo-c	81	20190610_FIRE_bh-w-mobo-c	81
20190610_Pauma_bh-w-mobo-c	80	20190610_Pauma_bh-w-mobo-m	80

Table 9: Scenes composed for target domain dataset by equation 2 (Part. 4)

Scene Description	# of Imgs	Scene Description	# of Imgs
20190620_FIRE_rm-w-mobo-c	81	20190715_MLOSouth1_lo-s-mobo-c	81
20190620_FIRE_smer-tcs9-mobo-c	72	20190715_MLOSouth2_lo-s-mobo-c	81
20190629_FIRE_hp-n-mobo-c	57	20190715_MLOSouth3_lo-s-mobo-c	81
20190712_CottonwoodFire_lp-s-mobo-c	81	20190716_FIRE_bl-s-mobo-c	70
20190712_FIRE_om-e-mobo-c	81	20190716_FIRE_mg-n-mobo-c	68
20190712_RockHouse_wc-e-mobo-c	79	20190716_FIRE_so-w-mobo-c	72
20190714_MLOSouth_lo-s-mobo-c	81	20190716_Meadowfire_hp-n-mobo-c	70
20190714_PinosSouth_pi-s-mobo-c	81	20190716_Riverfire_rm-w-mobo-c	80
20190717_FIRE_lp-n-mobo-c	81	20190717_FIRE_pi-w-mobo-c	81
20190728_Dehesa_lp-n-mobo	80	20190728_FIRE_om-n-mobo-c	79
20190728_FIRE_sp-n-mobo-c	81	20190801_Caliente_om-w-mobo	81
20190803_OtaySouth_lp-s-mobo	79	20190803_OtaySouth_om-s-mobo	79

Table 10: Scenes composed for target domain dataset by equation 2 (Part. 5)

Scene Description	# of Imgs	Scene Description	# of Imgs
20190803_Sage_om-n-mobo	73	20190814_FIRE_om-e-mobo-c	79
20190805_FIRE_sp-e-mobo-c	77	20190814_FIRE_pi-s-mobo-c	80
20190809_PinosSouth_pi-s-mobo	41	20190825_FIRE_smer-tcs8-mobo-c	80
20190810_SantaFire_rm-w-mobo	81	20190825_FIRE_sm-w-mobo-c	75
20190813_FIRE_69bravo-e-mobo-c	81	20190826_FIRE_pi-s-mobo-c	80
20190813_Topanga_69bravo-n-mobo	81	20190826_FIRE_rm-w-mobo-c	80
20190814_Border_lp-s-mobo	80	20190826_FIRE_smer-tcs9-mobo-c	80
20190827_FIRE_so-w-mobo-c	81	20190829_FIRE_bl-n-mobo-c	81
20190829_FIRE_pi-e-mobo-c	81	20190913_FIRE_lp-n-mobo-c	80
20190829_FIRE_rm-w-mobo-c	81	20190915_FIRE_rm-n-mobo-c	78
20190829_FIRE_smer-tcs8-mobo-c	76	20190922_FIRE_ml-w-mobo-c	81
20190924_FIRE_bl-s-mobo-c	79	20190924_FIRE_hp-s-mobo-c	80

Table 11: Scenes composed for target domain dataset by equation 2 (Part. 6)

Scene Description	# of Imgs	Scene Description	# of Imgs
20190924_FIRE_lo-w-mobo-c	79	20191001_FIRE_om-s-mobo-c	60
20190924_FIRE_lp-n-mobo-c	72	20191001_FIRE_rm-w-mobo-c	81
20190924_FIRE_ml-w-mobo-c	80	20191001_FIRE_smer-tcs9-mobo-c	80
20190924_FIRE_pi-w-mobo-c	79	20191003_FIRE_om-s-mobo-c	77
20190924_FIRE_sm-n-mobo-c	76	20191003_FIRE_rm-w-mobo-c	81
20190924_FIRE_wc-e-mobo-c	72	20191003_FIRE_smer-tcs9-mobo-c	77
20190924_FIRE_wc-s-mobo-c	70	20191005_FIRE_bm-e-mobo-c	79
20190925_FIRE_wc-e-mobo-c	81	20191005_FIRE_hp-s-mobo-c	81
20190925_FIRE_wc-s-mobo-c	81	20191005_FIRE_vo-n-mobo-c	77
20190930_FIRE_om-s-mobo-c	80	20191005_FIRE_wc-e-mobo-c	79
20191001_FIRE_bh-w-mobo-c	79	20191005_FIRE_wc-n-mobo-c	78
20191001_FIRE_lp-s-mobo-c	80	20191006_FIRE_lo-s-mobo-c	79
20191001_FIRE_om-e-mobo-c	79	20191006_FIRE_lo-w-mobo-c	80
20191006_FIRE_lp-e-mobo-c	72	20191006_FIRE_lp-n-mobo-c	73
20191006_FIRE_lp-s-mobo-c	73		

Table 12: Scenes composed for target domain dataset by equation 2 (Part. 7)

Scene Description	Imgs	Scene Description	Imgs
20191006_FIRE_ml-w-mobo-c	81	20200226_FIRE_rm-e-mobo-c	81
20191006_FIRE_om-n-mobo-c	78	20200304_FIRE_rm-w-mobo-c	81
20191006_FIRE_om-s-mobo-c	77	20200306_FIRE_mlo-n-mobo-c	81
20191006_FIRE_pi-s-mobo-c	78	20200306_FIRE_ml-s-mobo-c	81
20191007_FIRE_lp-s-mobo-c	81	20200306_FIRE_pi-n-mobo-c	81
20191007_FIRE_om-s-mobo-c	81	20200521_FIRE_om-n-mobo-c	81
20191007_FIRE_sm-s-mobo-c	81	20200521_FIRE_om-s-mobo-c	81
20191030_CopperCanyon_om-s-mobo-c	81	20200521_FIRE_om-w-mobo-c	81
20191030_CopperCanyon_om-s-mobo-m	81	20200521_VEGMGMT_bm-s-mobo-c	81
20200202_FIRE_hp-w-mobo-c	81	20200521_VEGMGMT_ml-w-mobo-c	81
20200205_FIRE_hp-w-mobo-c	81	20200521_VEGMGMT_wc-e-mobo-c	81
20200206_FIRE_ml-s-mobo-c	81	20200529_StructFire_wc-e-mobo-c	80
20200601_WILDLAND-DRILLS_mlo-e-mobo-c	81	20200608_FIRE_rm-w-mobo-c	81
20200601_WILDLAND-DRILLS_mlo-s-mobo-c	81	20200611_skyline_lp-n-mobo-c	81
20200601_WILDLAND-DRILLS_ml-s-mobo-c	81	20200614_DrumCanyon_syp-w-mobo-c	81
20200601_WILDLAND-DRILLS_om-e-mobo-c	81	20200615_Rainbow_rm-e-mobo-c	81

Table 13: Scenes composed for target domain dataset by equation 2 (Part. 8)

Scene Description	Imgs	Scene Description	Imgs
20200618_FIRE_om-w-mobo-c	81	20200727_Border11Fire_om-e-mobo-c	75
20200705_FIRE_bm-w-mobo-c	81	20200727_Border11Fire_om-e-mobo-m	75
20200705_FIRE_wc-n-mobo-c	81	20200806_BorderFire_lp-s-mobo-c	81
20200709_Tripp_hp-n-mobo-c	81	20200806_BorderFire_om-e-mobo-c	81
20200712_USSBonhommeRichard_sm-w-mobo-c	81	20200806_SpringsFire_lp-w-mobo-c	62
20200727_Border11Fire_lp-s-mobo-c	75	20200806_SpringsFire_lp-w-mobo-m	62
20200807_AppleFire-backfire-operation_hp-n-mobo-c	81	20200806_SpringsFire_om-n-mobo-c	65
20200808_OliveFire_wc-e-mobo-c	74	20200806_SpringsFire_om-n-mobo-m	62
20200812_LakeFire_dwpgm-n-mobo-c	81	20200806_SpringsFire_sm-e-mobo-c	65
20200813_Ranch2Fire_marconi-n-mobo-c	73	20200813_SkylineFire_sp-n-mobo-c	75
20200813_Ranch2Fire_sjh-n-mobo-c	78	20200813_VictoriaFire_lp-n-mobo-c	70
20200813_Ranch2Fire_wilson-e-mobo-c	77	20200822_BrattonFire_lp-e-mobo-c	81
20200822_BrattonFire_lp-s-mobo-c	81	20200828_BorderFire_om-w-mobo-c	80
20200822_SloaneFire_lp-n-mobo-c	81	20200828_BorderFire_sm-s-mobo-c	81
20200823_OakFire_pi-e-mobo-c	81	20200829_inside-Mexico_cp-s-mobo-c	81
20200829_inside-Mexico_mlo-s-mobo-c	81	20200831_FIRE_wc-n-mobo-c	180
20200905_ValleyFire_cp-s-mobo-c	0	20200905_ValleyFire_lp-n-mobo-c	73
20200905_ValleyFire_pi-w-mobo-c	75	20200905_ValleyFire_sm-e-mobo-c	71

Table 14: Scenes composed for target domain dataset by equation 2 (Part. 9)

Scene Description	Imgs	Scene Description	Imgs
20200911_FIRE_lp-e-mobo-c	81	20200930_inMexico_lp-s-mobo-c	81
20200911_FIRE_mlo-s-mobo-c	81	20200930_inMexico_om-e-mobo-c	81
20200911_FIRE_pi-s-mobo-c	81	20201003_structurefire_bh-w-mobo-c	80
20200930_BoundaryFire_wc-e-mobo-c	81	20201003_structurefire_bm-w-mobo-c	74
20200930_DeLuzFire_rm-w-mobo-c	61	20201013_FIRE_cp-s-mobo-c	79
20201105_Roundfire_lp-s-mobo-c	80	20201105_Roundfire_om-e-mobo-c	81
20201105_Roundfire_pi-s-mobo-c	81	20201127_Hawkfire_pi-w-mobo-c	81
20201202_BondFire-nighttime_sp-w-mobo-c	75	20201205_typical-range-fire_sclm-e-mobo-c	81
20201202_WillowFire-nighttime-near-CDF-HQ_lp-w-mobo-c	73	20201206_JEEP-ON-FIRE_om-w-mobo-c	70
20201202_WillowFire-nighttime-near-CDF-HQ_om-n-mobo-c	77	20201207_La_bh-s-mobo-c	81
20201202_WillowFire-nighttime-near-CDF-HQ_sm-n-mobo-c	77	20201208_FIRE_om-s-mobo-c	80
20201216_ChaparralFire_lp-w-mobo-c	81	20201216_ChaparralFire_om-n-mobo-c	81
20201216_ChaparralFire_pi-w-mobo-c	81		

Table 15: Scenes composed for target domain dataset by equation 2 (Part. 10)

B TRAINING DETAILS

In equation 3, L^S, L^M, L^A, L^C refers to supervised loss, masked image consistency loss (MIC loss), adversarial loss, and consistency loss each. More information could be seen in baseline method Hoyer et al. (2023) since we use same losses.

In the first source-only stage, we only used supervised learning. Our backbone is Resnet-50 with ImageNet pretrained weight. We trained 10 epoch with step decay learning rate schedule. We used 16 batch size, SGD optimizer with 0.9 momentum and 0.0005 weight decay.

In second stage, we also trained 10 epoch with same hyperparameter setup as first stage except that we used semi-supervised learning loss. We splitted image into 32x32 blocks and masked with ratio 0.5 for strong augmentation. We used 0.9 as EMA rate, and λ^M for 0.5. We used confidence score threshold as $\tau_u = 0.8, \tau_l = 0.05$. The final weight of first stage is used as initial weights. Overall hyperparameters used are summarized in Table 20.

$$\min_{\theta_s} \frac{1}{N_s} \sum_{k=1}^{N_s} L_k^S + \frac{1}{N_t} \sum_{k=1}^{N_t} (\lambda^M L_k^M) + \frac{1}{N_t + N_s} \sum_{k=1}^{N_t + N_s} (\lambda^A L_k^A + \lambda^C L_k^C) \quad (3)$$

C IMPACT OF USING BACKGROUND IMAGES FOR SEMI-SUPERVISED DOMAIN ADAPTATION

Background images are especially helpful for 0.5%, 1.0% protocols where pseudo labels with high confidence score is especially lacking as show in Table 21. We defined background image when there are no object with confidence score higher than 0.05.

Scene Description	# of Imgs	Scene Description	# of Imgs
20201216_ChaparralFire_sm-n-mobo-c	81	20210113_Borderfire_mlo-s-mobo-c	81
20201223_Creekefire_bh-w-mobo-c	81	20210113_Borderfire_pi-s-mobo-c	81
20210107_Miguelfire_om-w-mobo-c	80	20210115_Bonitafire_tp-w-mobo-c	71
20210110_Borderfire_lp-s-mobo-c	80	20210204_FIRE_tp-s-mobo-c	81
20210209_FIRE_hp-e-mobo-c	78	20210302_FIRE_lp-e-mobo-c	81
20210209_FIRE_tp-w-mobo-c	77	20210302_FIRE_lp-e-mobo-m	81
20210319_FIRE_om-n-mobo-c	81	20210711_FIRE_wc-e-mobo-c	81
20200906-BobcatFire-wilson-e-mobo-c	82	20210810-Lyonsfire-housefire-lp-n-mobo-c	64
20220210-EmeraldFire-marconi-w-mobo-c	82	20220210-EmeraldFire-signal-s-mobo-c	82
20220210-EmeraldFire-stgo-w-mobo-c	82	20220214-PrescribedFire-pi-n-mobo-c	82
20220302-Jimfire-0921-stgo-e-mobo-c	81	20220302-Jimfire-0921-stgo-s-mobo-c	81
20220302-Jimfire-1101-stgo-e-mobo-c	81	20220405-fire-in-Fallbrook-rm-s-mobo-c	81
20220405-fire-in-Fallbrook-rm-s-mobo-m	82	20220622-HighlandFire-wc-n-mobo-c	81
20220622-HighlandFire-wc-n-mobo-m	82	20220713-Lonestarfire-om-w-mobo-c	72
20220727-Casnerfire-bm-s-mobo-c	82	20220831-Border32fire-pi-s-mobo-c	65
20220831-Border32fire-pi-s-mobo-m	66	20220905-FairviewFire-bh-n-mobo-c	81
20220905-FairviewFire-smer-tcs3-mobo-c	82	20220905-FairviewFire-stgo-e-mobo-c	81
20220905-FairviewFire-tp-w-mobo-c	81	20221116-Willowfire-om-n-mobo-c	81
20221116-Willowfire-sm-n-mobo-c	81	20230128-Cardboard-Fire-om-w-mobo-c	82

Table 16: Scenes composed for target domain dataset by equation 2 (Part. 11)

Scene Description	# of Imgs	Scene Description	# of Imgs
rm-n-mobo-c	81	smer-tcs3-mobo-c	81
lp-e-iqeye	41	om-e-mobo-c	81
pi-s-mobo-c	81	ml-n-mobo-c	81
lp-n-iqeye	41	mg-s-iqeye	41
mw-e-mobo-c	81		

Table 17: Scenes composed for source domain dataset by only cameraName

Scene Description	# of Imgs	Scene Description	# of Imgs
bm-n-mobo-c	162	bl-n-mobo-c	243
rm-w-mobo-c	1193	bm-w-mobo-c	236
om-s-mobo-c	834	lp-s-iqeye	81
sm-n-mobo-c	628	pi-w-mobo-c	478
hp-n-mobo-c	694	bh-w-mobo-c	559
		bm-n-mobo	81

Table 18: Scenes composed for target domain dataset by only CameraName (Part 1.)



Figure 5: Example of our labeled dataset

D RELATION BETWEEN FOREGROUND-IMAGE AND BACKGROUND-IMAGE RATIO

Since there are dataset imbalance between label and unlabel images, we studied the best ratio between labeled and unlabeled data composing in a mini-batch. As shown in Table 22, 80% of unlabeled images used for minibatch had best result. It is as expected since the number of unlabeled images are more than 10 times than that of labeled dataset. We found that 90% unlabeled images used for mini-batch did not converged. We assume it is due to lack of supervisory signal in the early phase. We reported our result based on 80% of unlabel ratio in a mini-batch.

Scene Description	# of Imgs	Scene Description	# of Imgs
syp-n-mobo-c	81	syp-n-mobo-m	80
bl-e-mobo-c	243	bl-s-mobo-c	311
bm-s-mobo-c	227	sdsc-e-mobo-c	162
smer-tcs8-mobo-c	719	hp-e-mobo-c	159
mg-n-iqeye	81	so-s-mobo-c	81
bh-n-mobo-c	402	lo-s-mobo-c	565
tp-s-mobo-c	162	smer-tcs9-mobo-c	795
hp-w-mobo-c	243	rm-e-mobo-c	405
pi-e-mobo-c	405	rm-s-mobo	81
smer-tcs10-mobo-c	243	sp-s-mobo-c	153
sp-w-mobo-c	156	sm-w-mobo-c	237
ml-s-mobo-c	324	hp-s-mobo-c	229
wc-e-mobo-c	939	sm-e-mobo-c	217
lp-n-mobo-c	756	syp-w-mobo-c	243
sp-n-mobo-c	237	tp-e-mobo-c	81
sp-e-mobo-c	239	so-n-mobo-c	81
so-w-mobo-c	234	bh-s-mobo-c	323
mg-w-mobo-c	243	wc-n-mobo-c	572
mg-s-mobo-c	78	vo-w-mobo-c	81
sp-s-mobo-m	73	lp-s-mobo-c	874
om-n-mobo-c	704	bh-w-mobo-m	80
mg-n-mobo-c	68	lp-n-mobo	80
om-w-mobo	81	lp-s-mobo	159
om-s-mobo	79	om-n-mobo	73
pi-s-mobo	41	rm-w-mobo	81
69bravo-e-mobo-c	81	69bravo-n-mobo	81
ml-w-mobo-c	323	lo-w-mobo-c	159
wc-s-mobo-c	151	bm-e-mobo-c	79
vo-n-mobo-c	77	lp-e-mobo-c	315
sm-s-mobo-c	162	om-s-mobo-m	81
mlo-n-mobo-c	81	pi-n-mobo-c	163
om-w-mobo-c	546	mlo-e-mobo-c	81
mlo-s-mobo-c	324	lp-s-mobo-m	75
om-e-mobo-m	75	lp-w-mobo-c	297
lp-w-mobo-m	62	om-n-mobo-m	62
sm-e-mobo-m	63	dwpgm-n-mobo-c	81
marconi-n-mobo-c	73	sjh-n-mobo-c	78
wilson-e-mobo-c	159	cp-s-mobo-c	160
sclm-e-mobo-c	81	tp-w-mobo-c	229
lp-e-mobo-m	81	marconi-w-mobo-c	82
signal-s-mobo-c	82	stgo-w-mobo-c	82
stgo-e-mobo-c	243	stgo-s-mobo-c	162
rm-s-mobo-c	81	rm-s-mobo-m	82
wc-n-mobo-m	82	pi-s-mobo-m	66
smer-tcs3-mobo-m	82		

Table 19: Scenes composed for target domain dataset by only CameraName (Part 2.)

Table 20: Hyperparameters of training LADA with the proposed SSDA

Config	
Optimizer	SGD
Optimizer momentum	0.9
Weight decay	1e-4
Domain Adaptation rate	2.5e-3
Warmup epochs	0.333
Training epochs	10
EMA decay	0.9
τ_u	0.8
τ_l	0.05
λ^M	0.5
λ_{ins}^A	1e-1
λ_{img}^A	2.5e-2
λ_{ins}^C	1e-2
λ_{img}^C	2.5e-3

Table 21: LADA vs. baseline for ssda protocol

	ssda 0.5%	ssda 1.0%	ssda 3.0%
LADA(ours)	10.0	14.0	20.4
LADA(without background images)	7.9	13.9	20.9

Table 22: ratio between label vs. unlabel iamge in a minibatch

	0.5	0.6	0.7	0.8
SSDA-0.5%	25.2	27.2	27.0	27.3